Allosteric Regulation and Communication between Subunits in Uracil Phosphoribosyltransferase from *Sulfolobus solfataricus*[†,‡]

Susan Arent,[§] Pernille Harris,[§,||] Kaj Frank Jensen,[⊥] and Sine Larsen*[,§,#]

Centre for Crystallographic Studies, Department of Chemistry, University of Copenhagen, Universitetsparken 5, DK-2100 Copenhagen Ø, Denmark, Department of Chemistry, Technical University of Denmark, Kemitorvet, DK-2800 Kgs. Lyngby, Denmark, Department of Biological Chemistry, Institute of Molecular Biology, University of Copenhagen, Sølvgade 83H, DK-1307 Copenhagen K, Denmark, and European Synchrotron Radiation Facility, B.P. 220, 38043 Grenoble, France

Received September 10, 2004; Revised Manuscript Received October 27, 2004

ABSTRACT: Uracil phosphoribosyltransferase (UPRTase) catalyzes the conversion of 5-phosphate-α-1-diphosphate (PRPP) and uracil to uridine 5′-monophosphate (UMP) and diphosphate. The UPRTase from *Sulfolobus solfataricus* has a unique regulation by nucleoside triphosphates compared to UPRTases from other organisms. To understand the allosteric regulation, crystal structures were determined for *S. solfataricus* UPRTase in complex with UMP and with UMP and the allosteric inhibitor CTP. Also, a structure with UMP bound in half of the active sites was determined. All three complexes form tetramers but reveal differences in the subunits and their relative arrangement. In the UPRTase−UMP complex, the peptide bond between a conserved arginine residue (Arg80) and the preceding residue (Leu79) adopts a cis conformation in half of the subunits and a trans conformation in the other half and the tetramer comprises two cis−trans dimers. In contrast, four identical subunits compose the UPRTase−UMP−CTP tetramer. CTP binding affects the conformation of Arg80, and the Arg80 conformation in the UPRTase−UMP−CTP complex leaves no room for binding of the substrate PRPP. The different conformations of Arg80 coupled to rearrangements in the quaternary structure imply that this residue plays a major role in regulation of the enzyme and in communication between subunits. The ribose ring of UMP adopts alternative conformations in the cis and trans subunits of the UPRTase−UMP tetramer with associated differences in the interactions of the catalytically important Asp209. The active-site differences have been related to proposed kinetic models and provide an explanation for the regulatory significance of the C-terminal Gly216.

All organisms are able to synthesize pyrimidine nucleotides via *de novo* biosynthesis from compounds unrelated to nucleotides, but in addition, many organisms have biosynthetic salvage pathways that use preformed nucleosides and nucleobases to generate pyrimidine nucleotides. The nucleosides and nucleobases may be taken from the environment or produced endogenously by turnover of RNA. Using already formed nucleosides and nucleobases, the cell saves a significant amount of metabolic energy instead of using the *de novo* biosynthesis (*1*). Uracil phosphoribosyltransferase (UPRTase)[1] is a key enzyme in microbial pyrimidine salvage pathways. UPRTase catalyses the conversion of uracil and 5-phosphoribosyl-1-α-diphosphate (PRPP) to uridine monophosphate (UMP) in a Mg^{2+}-dependent reaction that releases diphosphate as the second product. The amino acid sequences of UPRTases are fairly dissimilar, with overall identities ranging from 20 to 45% but with strong conservation of the active-site residues (*2*). UPRTases have been identified in eubacteria, archaea, and lower eukaryotes,

[†] This work was supported by grants from the Danish National Research Foundation and the Faculty of Science, University of Copenhagen. We are grateful for the beam time provided at MAX-LAB Lund and EMBL/DESY Hamburg, for the financial support toward the travels to the synchrotrons provided by the EU under the Access to Research Infrastructures subprogram, and the Danish Natural Science Research Council contribution to Dansync.

[‡] The atomic coordinates and structure factors (PDB codes 1XTT, S.s.-UPRTase−UMP; 1XTU, S.s.-UPRTase−UMP−CTP; and 1XTV, S.s.-UPRTase−½UMP) have been deposited in the Protein Data Bank, Research Collaboratory for Structural Bioinformatics, Rutgers University, New Brunswick, NJ (http://www.rcsb.org/).

* To whom correspondence should be addressed. Telephone: +45 3532 0282 or +33 4 76 88 2181. Fax: +45 3532 0299 or +33 4 76 88 2160. E-mail: sine@ccs.ki.ku.dk or slarsen@esrf.fr.

[§] Centre for Crystallographic Studies, Department of Chemistry, University of Copenhagen.

[||] Technical University of Denmark.

[⊥] Department of Biological Chemistry, Institute of Molecular Biology, University of Copenhagen.

[#] European Synchrotron Radiation Facility.

[1] Abbreviations: PRTase, phosphoribosyltransferase; UPRTase, uracil PRTase or UMP synthase (EC 2.4.2.9); PRPP, 5-phosphoribosyl-1-α-diphosphate; PP_i, diphosphate; cPRPP, 1-α-pyrophosphoryl-2-α,3-α-dihydroxy-4-*β*-cyclopentanemethanol-5-phosphate; T.g.-UPRTase−GTP, crystal structure of *T. gondii* UPRTase in complex with GTP (PDB code 1JLR); T.g.-UPRTase−uracil−cPRPP, crystal structure of *T. gondii* UPRTase in complex with uracil and cPRPP (PDB code 1JLS); T.g.-apo-UPRTase, crystal structure of *T. gondii* apo-UPRTase (PDB code 1BD3); S.s.-UPRTase−UMP, crystal structure of *S. solfataricus* UPRTase in complex with UMP (PDB code 1XTT); S.s.-UPRTase−UMP−CTP, crystal structure of *S. solfataricus* UPRTase in complex with UMP and CTP (PDB code 1XTU); S.s.-UPRTase−½UMP, crystal structure of *S. solfataricus* UPRTase with half of the subunits occupied with UMP (PDB code 1XTV).

10.1021/bi048041l CCC: $30.25
Published on Web 12/30/2004

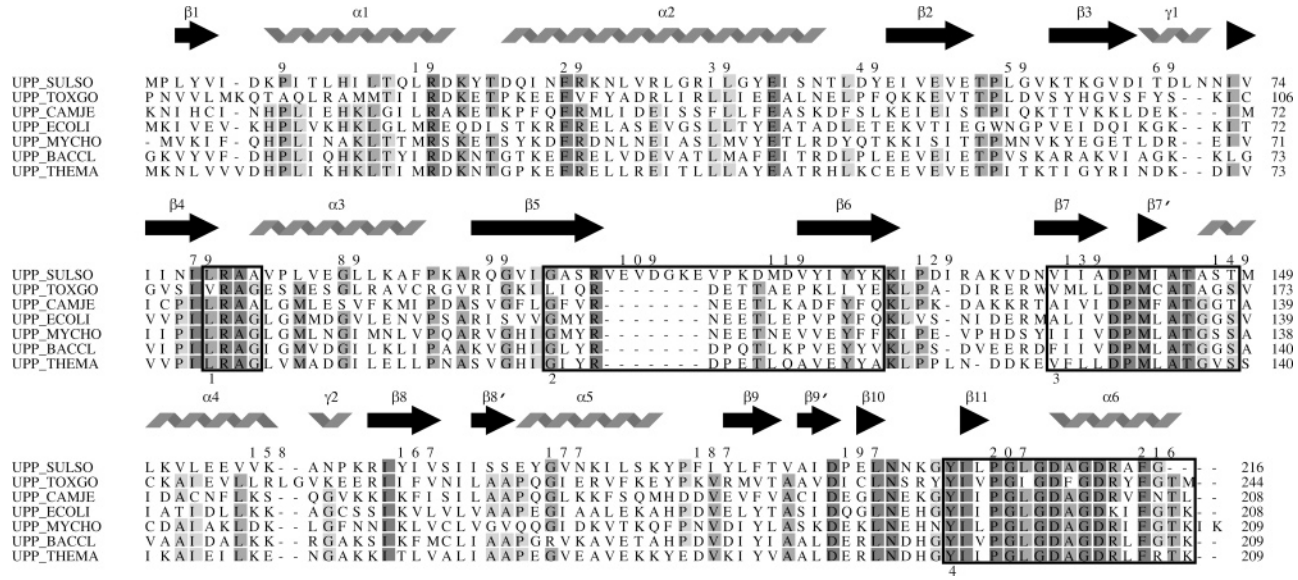

FIGURE 1: Alignment of the sequences of UPRTases from *S. solfataricus*, *T. gondii*, *Campylobacter jejuni*, *E. coli*, *Mycoplasma pulmonis*, *B. caldolyticus*, and *T. maritima*. The numbers refer to the sequence of the *S. solfataricus* UPRTase. Residues conserved in all seven sequences are shown with a dark gray background; identity in six sequences, with a gray background; and sequence identity in five sequences, with a light gray background. The secondary structural elements (twisted rods for α helices and arrows for β strands) for the *S. solfataricus* UPRTase are indicated above the sequences. Of the four boxes marked in the sequence alignment, the first three indicate residues involved in the PRPP binding and the last box surrounds residues involved in the binding of uracil.

while in mammals, the orotate phosphoribosyltransferase part of UMP synthase from the *de novo* biosynthetic pathway shows weak UPRTase activity (*3*).

The UPRTases from different organisms differ in their regulatory behavior. The enzymes from *Escherichia coli* and the eukaryotic parasite *Toxoplasma gondii* are activated by GTP, while the activity of the enzyme from *Bacillus caldolyticus* is unaffected by the presence of nucleoside triphosphates (*4*−*6*). For the *E. coli* and *T. gondii* enzymes, the effector molecule GTP reduces the concentration of PRPP needed for half-maximal reaction velocity by a factor of 5−7 but has no effect on V_{max}. The activation of these enzymes by GTP is associated with a change in their oligomeric state from a dimer to a tetramer. Both the activator molecule (GTP) and the substrate (PRPP) induce this change of quaternary structure, explaining why GTP only activates UPRTases at subsaturating concentrations of PRPP (*4*, *7*). Crystal structures are known for the UPRTases from *T. gondii* (*2*, *4*), *B. caldolyticus* (*8*), and *Thermotoga maritima* (*9*). The crystal structures of *T. gondii* UPRTase in complex with GTP (T.g.-UPRTase−GTP) and *T. gondii* UPRTase in complex with uracil and cPRPP (T.g.-UPRTase−uracil−cPRPP) revealed that the bound GTP and cPRPP make interactions with more than one dimer in the tetramer, explaining why binding of either of these ligands stabilizes the tetramer (*4*). Like all other phosphoribosyltransferases from *de novo* and salvage pathways for biosynthesis of pyrimidine and purine nucleotides, the UPRTases belong to the structurally well-characterized PRT family (*10*).

The UPRTase from *S. solfataricus* differs significantly from the other UPRTases investigated with respect to its regulation. GTP binding does not change the oligomeric state; it increases the catalytic velocity k_{cat} by approximately 20-fold, while K_m for PRPP is almost unaffected, K_m for uracil increases more than 10-fold, and the activating effect of GTP cannot be eliminated by increasing the concentration of PRPP (*11*). This is a behavior that differs significantly from the one described earlier for the *E. coli* and *T. gondii* UPRTases, also regulated by GTP. Also, with respect to its inhibition, the *S. solfataricus* UPRTase differs from other UPRTases. Both the reaction product UMP and the allosteric effector CTP inhibit this UPRTase. Neither UMP nor CTP are strong inhibitors individually under activating conditions (i.e., high PRPP and GTP concentrations), but the inhibition is efficiently enhanced when both UMP and CTP are present. Furthermore, kinetic investigations had lead to the proposition that the C terminus plays an important role in its regulation.

UPRTase has attracted attention as a potential drug target, because this enzyme from the pyrimidine salvage pathway is lacking in mammals (*2*). The variation in reactivity and regulation displayed by UPRTases from different organisms made it attractive to investigate the structural origins for the unique regulatory behavior of UPRTase from *S. solfataricus*. Analysis of the UPRTase sequences did not lead to any suggestions of residues that could play a role for the differences in regulatory behavior of the *S. solfataricus* UPRTase (Figure 1). Seven additional amino acids in the region corresponding to the flexible loop covering the active site represent the most pronounced difference. It suggests that the UPRTase from *S. solfataricus* has a significantly longer flexible loop than the UPRTases found in other organisms.

To elucidate the enzymatic function of the *S. solfataricus* UPRTase, we determined the crystal structures for three different nucleotide complexes of the enzyme. Analysis of these structural results enabled us to provide a structural explanation of the unique allosteric regulation of the *S. solfataricus* UPRTase. The conformational changes and rearrangement of the quaternary structure revealed by the analysis provided the basis to propose a structural model for the communication between the binding site for the allosteric regulators and the active-site pocket.

MATERIALS AND METHODS

Expression and Purification. Recombinant UPRTase from *S. solfataricus* was purified following the previously described procedure (*11*). The protein samples used for crystallization were pure according to SDS−PAGE and isoelectric-focusing gel-electrophoresis analyses. The enzyme prepared this way has UMP bound despite several column chromatography steps and dialysis during purification (*11*). The enzyme was stored at 193 K at a concentration of approximately 17 mg/mL in 10 mM Tris-HCl at pH 8.0, 0.1 mM EDTA, and 10% (v/v) glycerol.

For the production of selenomethionine-substituted *S. solfataricus* UPRTase, the gene was expressed in the methionine auxotroph *E. coli* K12 strain SØ 6735 (*metA*, *rph-1*, *recA56 srlC300*::Tn*10* [F′*lacI*^{q1} *lacZ*::Tn5]), a derivative of *E. coli* strain DL41 (*E. coli K12 metA*, *rph-1*), which has previously been used for preparation of selenomethionine-substituted proteins (*12*, *13*). The starter culture was grown at 310 K in AB medium (*14*) supplemented with 0.5% glucose, 4 μg mL^{-1} thiamine, 40 μg mL^{-1} uracil, 100 μg mL^{-1} ampicilin, and 50 μg mL^{-1} L-methionine. The cells were harvested by centrifugation in the exponential growth phase and resuspended to an OD_{436} of 0.1 in prewarmed medium of the same type but with 100 μg mL^{-1} D,L-selenomethionine replacing L-methionine. Protein synthesis was induced by the addition of 0.5 mM isopropyl-β-D-thiogalactoside when the OD_{436} of the culture was 0.9. The culture was grown to stationary phase overnight.

The selenomethionine-substituted UPRTase was purified as the native UPRTase (*11*). The activity, the GTP activation, and the thermostability of the selenomethionine-substituted enzyme were comparable with the corresponding parameters of the native enzyme (data not shown).

Crystallization. Crystal Screen I from Hampton Research (*15*) was used for initial screening of crystallization conditions by vapor diffusion in hanging drops. Each drop, made of 2 μL of protein solution (5 mg/mL UPRTase) mixed with 2 μL of reservoir solution, was suspended on a siliconized cover slip over 1 mL of reservoir solution. Crystals grown by vapor diffusion appeared under several conditions within 1 day of equilibration at room temperature. Crystals of *S. solfataricus* UPRTase complexed with UMP (S.s.-UPRTase−UMP) were obtained with a reservoir solution containing 13% (w/v) poly(ethylene glycol) 4000 and 500 mM sodium acetate at pH 5.5. Crystals of selenomethionine-substituted S.s.-UPRTase−UMP were obtained with the reservoir solution 16.5% (w/v) poly(ethylene glycol) 8000, 500 mM sodium acetate, and 300 mM morpholine ethanesulfonic acid at pH 6.5. Before crystallization, 2.5 mM tris(2-carboxyethyl)phosphine hydrochloride was added to the solution of the selenomethionine-substituted protein to prevent oxidation of selenomethionine and 1 mM UMP was added to ensure product saturation of the enzyme. Crystals of *S. solfataricus* UPRTase in complex with UMP and CTP were obtained adding 1 mM CTP, 3 mM $MgCl_2$, and 1 mM UMP to the protein solution before setup of the drops against a reservoir solution containing 24% (w/v) poly(ethylene glycol) 4000, 200 mM $MgCl_2$, and 100 mM Tris-HCl at pH 8.0. The crystals of a third complex were obtained by equilibrating drops made of a protein solution mixed with 1 mM GTP and 3 mM $MgCl_2$ against a reservoir solution 3.2 M sodium formate with 10% (v/v) glycerol.

Data Collection and Processing. The UPRTase crystals were soaked in mother liquor containing 10−13% (v/v) glycerol before flash cooling in liquid nitrogen. X-ray diffraction data on single crystals cooled to 100 K of the three native UPRTase-complexes data were collected using an imaging plate or a CCD detector from MAR Research at beamline I711, MAX-lab, Lund University, Sweden (*16*). The wavelength for all three experiments was close to 1 Å. Beamline BW7A, EMBL Hamburg outstation DESY, was employed for the data collection for the selenomethionine-substituted S.s.-UPRTase−UMP complex on a crystal cooled to 100 K. The wavelength used for the data collection corresponded to the absorption peak of the selenium K edge. Auto indexing, data reduction, and scaling were performed with programs from the HKL suite (*17*). The structure factors were derived from the reflection intensities using TRUNCATE (*18*). A summary of the data reductions are contained in Table 1.

Structure Determinations. The structure of *S. solfataricus* UPRTase in complex with UMP (S.s-UPRTase−UMP) was determined by the single-wavelength anomalous dispersion method using data collected from a crystal of the selenomethionine-substituted protein. With SOLVE (*19*), it was possible to locate 11 of the expected 12 selenium atoms in the asymmetric unit, 3 from each of the 4 subunits. The missing selenium atom was localized using SHARP (*20*), which also was employed in the refinement of the positions for all 12 selenium atoms. The 2-fold noncrystallographic symmetry relating the 12 selenium atoms was identified using RESOLVE (*21*), which also was used for subsequent density modifications and averaging of the electron-density map. It was possible to fit the core region of UPRTase from *T. gondii* into this averaged electron-density map and manually rebuild the structure with the program O (*22*). New maps were calculated using the phases from this initial model in combination with the experimental phases, and the remaining parts of the structure were easily built. The native data set to a resolution of 1.8 Å was subsequently used for the structure refinement. Refinement of the structure was carried out with CNS (*23*) using the automatic procedure for water insertion. In half of the subunits of the S.s-UPRTase−UMP structures, the peptide bond between Leu79 and Arg80 adopts a cis conformation, clearly shown from the fit of the two amino acids into the electron density in the $2F_o - F_c$ maps. The four independent subunits in the asymmetric unit were refined without any NCS restraints.

The two other complexes form triclinic crystals with two tetramers in the unit cell. Their structures were determined by the molecular-replacement method using AMoRe (*24*), using the S.s.-UPRTase−UMP dimer as the search model. In the *S. solfataricus* UPRTase complex with UMP and CTP (S.s.-UPRTase−CTP−UMP) it was found that the best fit to the electron density is achieved when the Leu79-Arg80 peptide bond is in a trans conformation. The structure determination for the crystals formed in the presence of GTP revealed that no GTP was bound, whereas UMP was bound in only half of the subunits. The lack of GTP in these crystals can be explained by the high concentration of sodium formate present during crystallization. This structure (S.s.-UPRTase−

Table 1: Data Collection and Refinement Statistics

enzyme	SeMet	wild type	wild type	wild type
complex	S.s-UPRTase−UMP	S.s-UPRTase−UMP	S.s-UPRTase−UMP−CTP	S.s-UPRTase−$^1/_2$UMP
crystal parameters				
space group	$P2_1$	$P2_1$	$P1$	$P1$
a (Å)	59.0	58.8	71.7	68.1
b (Å)	96.6	97.5	76.5	73.6
c (Å)	73.5	73.4	91.5	115.1
α (deg)	90.0	90.0	109.0	85.8
β (deg)	93.5	93.7	90.8	85.3
γ (deg)	90.0	90.0	115.4	62.5
number of subunits per asu	4	4	8	8
data collection statistics				
resolution range[a] (Å)	25−2.35 (2.39−2.35)	25−1.8 (1.83−1.80)	25−2.8 (2.91−2.80)	25−2.6 (2.69−2.60)
number of observations	322 685	344 026	88 654	101 199
number of unique reflections	35 496	76 607	40 931	60 659
mosaicity (deg)	1.0	0.6	1.8	1.1
R_{merge}	0.100 (0.233)	0.142 (0.410)	0.116 (0.450)	0.098 (0.397)
completeness	0.960 (0.787)	0.942 (0.909)	0.985 (0.977)	0.914 (0.797)
$I/\sigma(I)$	13.1 (3.5)	12.7 (3.3)	6.6 (1.9)	6.8 (1.3)
refinement statistics				
number of reflections used in R		72 058	39 575	55 369
number of reflections used in R_{free}		1758	1961	1438
R		0.193 (0.247)	0.222 (0.357)	0.227 (0.358)
R_{free}		0.228 (0.274)	0.257 (0.350)	0.263 (0.367)
rmsd for bond lengths (Å)		0.005	0.008	0.008
rmsd for bond angles (deg)		1.3	1.3	1.3
Ramachandran plot (% in allowed, generously allowed, and disallowed regions)		99.5, 0.5, 0	98.5, 1.5, 0	99.3, 0.7, 0
number of atoms (protein, ligands, water)		6674, 92, 692	13 560, 400, 0	13 560, 84, 0
average B factors (Å^2) (protein, ligands, water)		19, 15, 29	41, 60	32, 28

[a] The numbers in parentheses refer to the outermost resolution shell.

$^1/_2$UMP) was determined to 2.6 Å resolution, and in all eight subunits, the peptide bond between Leu79 and Arg80 was assigned as trans. Refinement of these two structure was also performed with CNS (*23*). For the S.s.-UPRTase−CTP−UMP structure, restrained NCS was imposed on all eight subunits. For the S.s.-UPRTase−$^1/_2$UMP structure, restrained NCS symmetry was imposed between the two tetramers, while no restraints were imposed between the subunits in the tetramer. The final refinement statistics for the three structures are shown in Table 1. The quality of the structures was examined with PROCHECK (*25*), and no residues were found in the disallowed regions of the Ramachandran plot (Table 1). The illustrations in Figures 2 and 3 were prepared using MOLSCRIPT (*26*) and Raster3D (*27*). Sequence alignment was performed using the INDONESIA program package (http://xray.bmc.uu.se/∼dennis) (*28*).

RESULTS

Crystal Structures. The crystal structures were determined for three complexes of the *S. solfataricus* UPRTase. The three structures revealed that the enzyme is a tetramer irrespective of the nature and number of the bound nucleotides, in agreement with the oligomeric state of the enzyme in solution (*11*). The structure determined to the highest resolution (1.8 Å) has UMP bound in all four subunits (S.s.-UPRTase−UMP) representing a partly inhibited form of the enzyme. The structure of the fully inhibited enzyme, i.e., *S. solfataricus* UPRTase with UMP and CTP bound to all subunits (S.s.-UPRTase−UMP−CTP), was determined to 2.8 Å resolution. The third crystal structure with UMP bound to only two of the four subunits in the tetramer (S.s.-UPRTase−$^1/_2$UMP) was determined to 2.6 Å resolution. The three structures show good geometry, with more than 98% of the residues in the allowed regions of the Ramachandran plot and no residues in the disallowed regions (Table 1).

The S.s.-UPRTase subunits in the three structures adopt an overall fold (Figure 2A) that conforms well with the other known UPRTase structures. Its core comprises the PRT fold (*10*) consisting of a five-stranded, parallel β sheet (β_5-β_4-β_7-β_8-β_9) sandwiched between α helices. In the UPRTases, the sheet has three helices (α_1, α_2, and α_3) on one side and two (α_4 and α_5) on the other side. The central β sheet is flanked by the antiparallel β_6 strand connected to β_5. The flexible loop between β_5 and β_6 is significantly longer in the *S. solfataricus* UPRTase. It is one of the regions in the sequence (Box 2 in Figure 1) that is known to play a role in the binding of the substrate PRPP. The two other regions interacting with PRPP are boxed in Figure 1. These are the small PP_i-binding loops (between β_4 and α_3), with the key element of PRPP recognition, namely, a nonproline cis peptide bond between its first and second residue (*10*) and the PRPP recognition motif. The third box marks the PPRP recognition motif, which is conserved with characteristic variations for the members of the PRT protein family (*29*). Another characteristic of the PRT protein family is the small subdomain on top of the central β sheet known as the hood. In the UPRTases, it is comprised of two short antiparallel β strands (β_{10} and β_{11}) and the α_6 helix. The hood is involved in substrate recognition mainly through backbone interactions and hosts the binding site for uracil.

A structural feature unique for the UPRTases is the β arm formed by the antiparallel β strands, β_2 and β_3, that extend

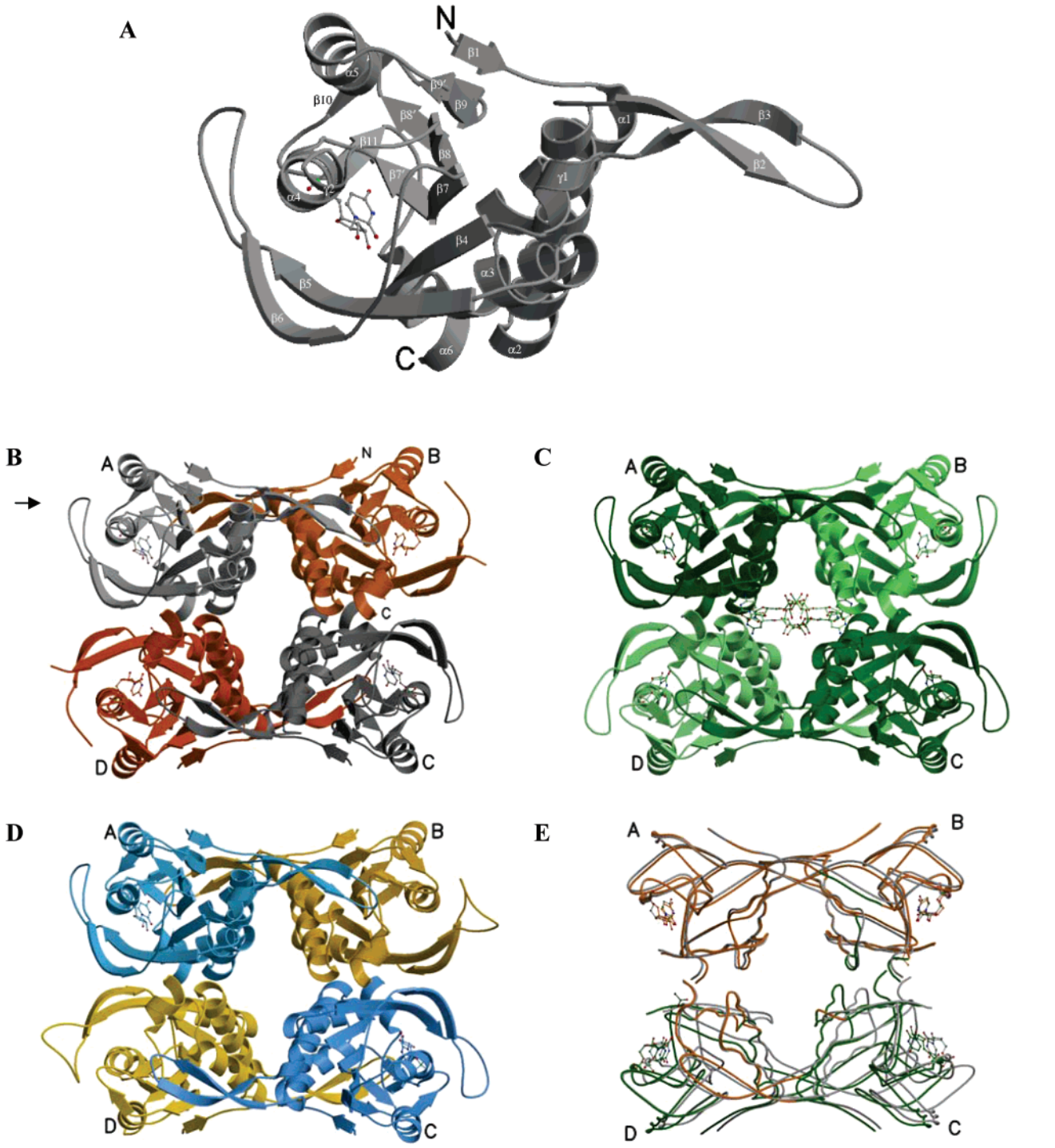

FIGURE 2: Ribbon diagrams of the *S. solfataricus* UPRTase. (A) Cis subunit from the S.s.-UPRTase−UMP oriented like the subunit A in the three tetramer structures shown in B−D. Similar subunits are represented by similar colors. (B) S.s.-UPRTase−UMP with four UMP molecules, represented as a ball-and-stick model, bound in the active sites. The arrow is pointing at the tip of the flexible loop in subunit A. The cis subunits are illustrated in gray colors, and the trans subunits are illustrated in orange. (C) S.s.-UPRTase−UMP−CTP with four UMP molecules in the active sites and four CTP molecules at the dimer−dimer interface represented as a ball-and-stick model. (D) S.s.-UPRTase−$^1/_2$UMP, the UMP molecules in two of the active sites are drawn as a ball-and-stick model. The subunits with UMP bound are given in blue colors. (E) Rearrangement of the quaternary structure upon binding of CTP. S.s.-UPRTase−UMP−CTP is colored in gray. S.s.-UPRTase−UMP is color-coded according to the segments; segment 1 is superposed and colored in orange and segment 2 is colored in green.

from the core. The residues in the β arm make interactions with the adjacent subunit, and the β arm seems to be important for dimer stabilization. Leu58 at the tip of the β arm from the other subunit in the dimer is close to the active site. The separation between the two active sites in the dimer is approximately 49 Å, measured as the distance between the backbone carbonyl oxygens of Gly208, while the separation between an active site in one dimer and the nearest active site in the other dimer is approximately 35 Å.

The individual subunits of the *S. solfataricus* UPRTase structures show some remarkable differences. The refinement of the S.s.-UPRTase−UMP structure revealed that, although

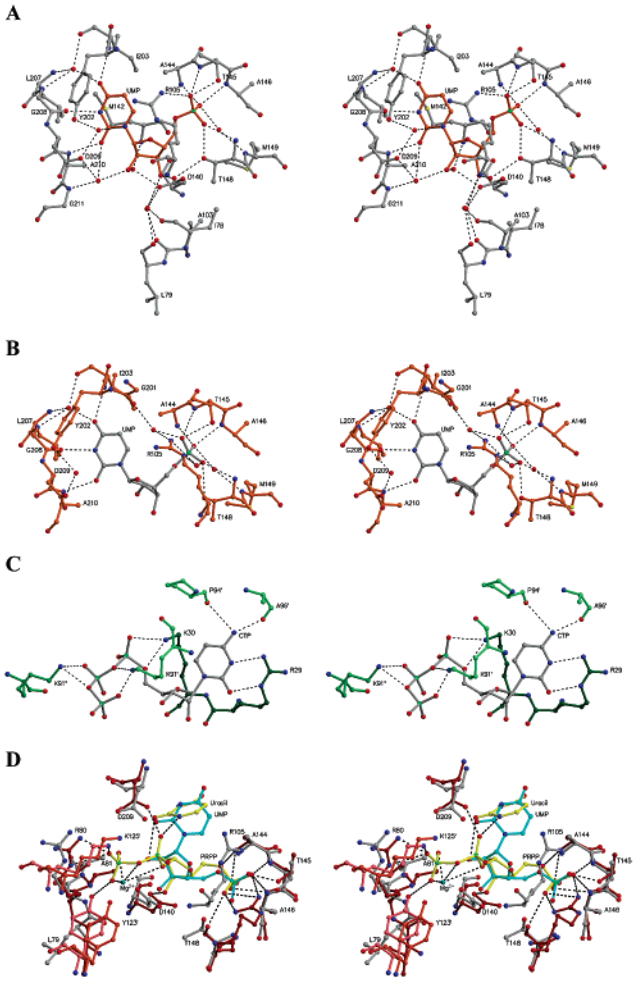

FIGURE 3: Illustrations of the binding of nucleotides to S.s.-UPRTase. Residues from different subunits are represented by different colors. (A) Stereoview of the binding of UMP in the cis subunits of S.s.-UPRTase−UMP. (B) Stereoview of the UMP binding in the trans subunits of S.s.-UPRTase−UMP. (C) Stereoview of CTP binding in S.s.-UPRTase−UMP−CTP illustrating the hydrogen bonds between CTP and residues from three different subunits. (D) Superposition of T.g.-UPRTase−uracil−cPRPP (pink, red, and yellow) and S.s.-UPRTase−UMP (gray, orange, and cyan).

all subunits have UMP bound, the Leu79-Arg80 peptide bond in the PP_i-binding loop is in a cis conformation in half of the subunits and in a trans conformation in the other half. A similar breaking of symmetry is seen in the S.s.-UPRTase−$^1/_2$UMP structure, where UMP is only bound to half of the subunits; in this structure, all of the Leu79-Arg80 peptide bonds are in a trans conformation. The S.s.-UPRTase−CTP−UMP structure is the only tetramer with four identical subunits that all have the Leu79-Arg80 peptide bond in a trans conformation. It is obvious that these differences in the subunits influence the interactions and the quarternary structure of the *S. solfataricus* UPRTase.

Differences in the Quarternary Structure. Superficially, the tetrameric arrangement observed in the three complexes looks the same. However, the quaternary structures of the three *S. solfataricus* UPRTase complexes are distinctively different. Figure 2B shows the tetramer found in S.s.-UPRTase−UMP, where the subunits are related by 2-fold symmetry. In the gray subunits labeled with A and C, the peptide bond between Leu79 and Arg80 is in a cis conformation (cis subunits), and in the orange subunits labeled B and D, the same peptide bond is in a trans conformation (trans subunits). The cis and trans subunits are interacting through their dimer arms forming a tight asymmetric (cis−trans) dimer (A−B and C−D) (Figure 2B). In addition, the asymmetry of the dimer is reflected in the binding of UMP *vide infra* and in the conformation of the flexible loop, which is ordered in the cis subunits and highly mobile with disorder in the trans subunits. The electron density was so poorly defined that it was impossible to include seven residues at the tip of the flexible loop (B107−B113 and D107−D113) in the model. The differences between the subunits lead to differences in the hydrogen-bond networks that connect the subunits in the tetramer. The cis and trans subunits contribute with different residues in the formation of hydrogen bonds across the equivalent A−D and B−C interfaces. Superposition of the cis and trans subunit shows the expected discrepancy in the PP_i loop caused by the difference in conformation of the peptide bond between the first (Leu79) and second (Arg80) residue of the PP_i loop.

In contrast, the S.s.-UPRTase−UMP−CTP tetramer is composed of four identical subunits (Figure 2C). The subunit of the S.s.-UPRTase−UMP−CTP tetramer superposes well with the cis subunit in S.s.-UPRTase−UMP, except in the PP_i loop. The modest data resolution for the S.s.-UPRTase−UMP−CTP structure makes it impossible to determine the conformation of the Leu79-Arg80 peptide bond unambiguously. It is clear, however, that it differs from the main-chain conformation around the peptide bond in both the cis and trans subunits in the S.s-UPRTase−UMP complex.

The S.s-UPRTase−$^1/_2$UMP structure shows an asymmetry that is similar to the one displayed in the S.s.-UPRTase−UMP structure. In this case, the difference is caused because UMP is bound to only half of the subunits. The S.s-UPRTase−$^1/_2$UMP tetramer is made up of four slightly different subunits, which are similar in pairs of two (Figure 2D). The subunit with UMP bound superposes well with the cis subunit in S.s.-UPRTase−UMP. Although the subunit without UMP has an ordered flexible loop, it does not show a recognizable similarity with the flexible loop in either the cis or trans subunit. The variation in the quaternary structure must be related to the differences in the nucleotide binding, and we examine this aspect more closely in the following paragraph.

Nucleotide Binding in the Three Complexes. The asymmetry of the cis−trans dimer is reflected in interactions between the protein and the bound nucleotide. Figure 3A illustrates how UMP is bound in the cis subunits of the S.s.-UPRTase−UMP structure, and Figure 3B illustrates the UMP binding in the trans subunits. It is obvious that uracil and the 5′ phosphate are interacting with the same residues in the two sites, whereas the ribose ring is positioned differently. This difference is accompanied by a decrease in the number of water-mediated hydrogen bonds connecting the protein and the ribose ring in the trans subunit compared to the cis subunit and differences in the conformation of the conserved residues in the active site. The most interesting is the change for the proposed catalytic residue Asp209 (*8*). The significance of this residue for the function of UPRTases was demonstrated by mutation of the corresponding aspartate residue in *T. gondii* to an alanine residue, which resulted in an inactive enzyme (*4*). In the cis subunit, the carboxylate

of Asp209 interacts both with uracil and the ribose ring via two water molecules, while these interactions are lost in the trans subunit. Apparently, the conformation of the bound product UMP depends on the number of interactions and therefore on the conformation of the Leu79-Arg80 peptide bond.

The binding of CTP to *S. solfataricus* UPRTase results in a rearrangement of the quarternary structure from a tetramer composed of two asymmetric cis−trans dimers to a homotetramer with four identical subunits. Furthermore, CTP binding and the accompanying rearrangement of the tetramer stabilizes the flexible loop in a closed conformation. The four CTP molecules are bound at the interface between the two dimers, and residues from three subunits of the tetramer make interactions with each inhibitor molecule as shown in Figure 3C. The triphosphate moieties of the CTP molecules point toward each other, which suggests that they are neutralized by a counterion whose nature and position cannot be identified because of the limited data resolution.

DISCUSSION

Rearrangement of the Quaternary Structure. *T. gondii* UPRTase changes its oligomeric state from a dimer to a tetramer in solution upon binding of either PRPP or GTP, while the crystal structures of different nucleotide complexes are all identical homotetramers, which superpose well (*2*, *4*). In contrast, we find that the tetramers of S.s-UPRTase−UMP and S.s.-UPRTase−UMP−CTP do not superimpose well. To describe the apparent change in the quaternary structure between these two tetramers, we used Hingefind (*30*) in a search for invariant segments and their relative movements, excluding residues in the flexible loop region (102−128). The search resulted in the detection of two segments within the tetramer (Figure 2D). Segment 1 is comprised of residues 2−51, 56−102, and 128−216 from subunit A, residues 2−19, 29−102, and 128−211 from subunit B, residues 50−66 and 94−95 from subunit C, and residues 12−33, 82−88, and 207−216 from subunit D. Segment 2 contains the remaining residues. The analysis showed that segment 1 in S.s.-UPRTase−UMP superposes well with segment 1 in S.s.-UPRTase−UMP−CTP (Figure 2D) and that superposition of segment 2 in the two tetramers can be obtained by rotating the S.s.-UPRTase−UMP tetramer 6° with respect to the S.s.-UPRTase−UMP−CTP tetramer. This implies that the rearrangement of the quaternary structure caused by binding of CTP to all subunits can be described as a 6° rotation of segment 2 with respect to segment 1.

The change in quarternary structure affects the interface between the two dimers. Slightly more of the surface area is buried in the S.s.-UPRTase−UMP−CTP tetramer (14%) relative to the S.s.-UPRTase−UMP tetramer (11%). It is noteworthy that the CTP binding does not influence the interface between subunit A and B, whereas there are changes of the hydrogen bonds connecting subunits A and D (B and C).

PRPP Binding. To get information about the binding of PRPP, we have superposed the S.s.-UPRTase−UMP structure with the structure of *T. gondii* UPRTase in complex with the substrate analogue cPRPP (*4*). The structure of the cis subunit in S.s.-UPRTase−UMP superposes very well with the subunits of UPRTase from *T. gondii*, while the cis−trans dimer has a different twist from the dimers in the *T. gondii* UPRTase and cannot be superposed as a whole. Figure 3D shows a superposition of the uracil−cPRPP binding site in the T.g.-UPRTase−uracil−cPRPP structure with the UMP-binding site in the cis subunit of the S.s.-UPRTase−UMP complex. All residues forming the binding site are either conserved or replaced with residues with side chains of similar functionality. The conserved interactions involve Tyr123 and Lys125, which form hydrogen bonds to the β-phosphate oxygen of cPRPP across the dimer−dimer interface. The equivalent superposition of the trans subunit in S.s.-UPRTase−UMP shows that the trans conformation of the Leu79-Arg80 peptide bond causes the side chain of Arg80 to occupy the space where cPRPP is located in the T.g.-UPRTase−uracil−cPRPP complex. The steric hindrance exerted by Tyr123 and Lys125 from the adjacent subunit prevents Arg80 from adopting the same position as in the cis subunit of S.s.-UPRTase−UMP and T.g.-UPRTase−uracil−cPRPP. Consequently, a rearrangement of the binding site in the trans subunit structure is required before or during the binding of PRPP. For the *T. gondii* enzyme, no conformational changes can be detected from the comparison of the T.g.-UPRTase−uracil−cPRPP and T.g.-apo-UPRTase structures. The comparison to the *T. gondii* UPRTase structures suggests that binding of PRPP to *S. solfataricus* UPRTase is associated with internal structural changes, while the PRPP binding in *T. gondii* induces a change of its oligomeric state.

Differences in the Conformation of UMP. Superposition of the two subunits in the asymmetric cis−trans dimer of S.s.-UPRTase−UMP reveals a difference in the orientation of the ribose group of bound UMP, while the pyrimidine base and the 5′ phosphate are at the same positions. The two different conformations of UMP indicate that the two active sites represent different states of the reaction. The ribose conformation in the cis subunit is similar to the conformation of ribose in the substrate analogue cPRPP in the T.g.-UPRTase−uracil−cPRPP structure. This means that UMP is in a strained conformation supported by numerous interactions with the protein, when the peptide bond between Leu79 and Arg80 is in a cis conformation (Figure 3A). On the other hand, the conformation of UMP in the trans subunit of S.s.-UPRTase−UMP corresponds to the one observed in the small molecule crystal structure of its sodium salt (*31*). Apparently, this relaxed conformation of UMP is coupled with the occurrence of a trans conformation of the peptide bond between Leu79 and Arg80 and a reduced number of interactions with the protein (Figure 3B). From this, we conclude that there is a reduced amount of energy stored in the trans subunit compared with the cis subunit in S.s.-UPRTase−UMP. When S.s.-UPRTase−$^1/_2$UMP is included in the comparison, a third step may be integrated in the analysis. The subunit without UMP bound in this complex, which is the closest that we could approach an apoenzyme, may represent the state between two cycles of catalysis. In this subunit, Arg80 is in a position similar to the position of Arg80 in S.s.-UPRTase−UMP−CTP (*vide infra*), suggesting that Arg80 rearranges during the binding of PRPP.

For pyrimidine and purine PRTases, it has been recognized that nucleophilic substitution by electrophile migration is part of the enzymatic mechanism (*32*−*34*). This mechanism is a

nucleophilic-substitution reaction in which both attacking- and leaving-group nucleophiles are held tightly in their respective binding pockets and the C1′ carbon of the ribose ring translates between the relatively immobile nucleophiles during catalysis. The different conformations that UMP adopts in the active sites support the fact that UPRTase utilizes an equivalent mechanism for ribosyl migration.

The characterization of the active sites in the *S. solfataricus* UPRTase in complex with UMP reveals three different active-site structures, and it was attractive to examine if they could be related to different steps in catalysis. The kinetic behavior observed for *S. solfataricus* implies that an isomerization step follows PRPP binding (*11*), where the proposed isomerization corresponds to a change of the enzyme−PRPP Michaelis complex to a form of the complex that is able to bind uracil. The structures of the "apo" subunit in S.s.-UPRTase−$^1/_2$UMP and the cis subunit in S.s.-UPRTase−UMP support this interpretation of the kinetic results, because isomerization of the Arg80 side chain and of the peptide bond between Leu79-Arg80 has to occur between the two steps in the catalysis. For completion of the catalytic cycle and release of the last product, the enzyme has to reverse the isomerization reaction. This last step is also supported by our structural results. The two different subunits in S.s.-UPRTase−UMP show that the conformational change of Arg80 side chain and the isomerization of the Leu79-Arg80 peptide bond take place before the release of the product UMP.

Conserved Residue Arg80 Plays a Key Role in Inhibition by CTP. In the S.s-UPRTase−UMP−CTP structure, the side chain of Arg80 is positioned at the place occupied by the cPRPP molecule in T.g.-UPRTase−uracil−cPRPP complex and Arg80 is not able to adapt the same conformation as in the cis subunit of S.s-UPRTase−UMP because of sterical hindrance from Phe215 of the same subunit and Val100 and Tyr123 from the other subunit across the dimer−dimer interface (Figure 4A). Binding of CTP thus results in structural changes, which leave no room for the binding of PRPP. This may explain the competitive nature of PRPP and CTP binding observed in ligand-binding assays (*11*). The position of the Arg80 side chain is the only difference observed between the UMP-binding site in the cis subunit of S.s.-UPRTase−UMP and S.s.-UPRTase−UMP−CTP. The changed position of Arg80 does not result in any extra direct interactions with UMP, which is in agreement with the binding constant for UMP being unaffected by the presence of CTP (*11*). An explanation of the cooperative inhibition by UMP and CTP could be that movement of the flexible loop covering the active site is necessary for product release, because the flexible loop is apparently stabilized by the binding of CTP and the accompanying arrangement of the quaternary structure. The fact that the release of the product may well be the rate-limiting step in catalysis by *S. solfataricus* UPRTase is in line with what is observed for other PRTases (*35*−*37*).

Effect and Binding of GTP. The GTP-binding site in T.g.-UPRTase−GTP is located between the beginning of the flexible loop and the beginning of the loop in the β arm involved in dimer stabilization (*4*). This location is one of the few regions that is not conserved between *T. gondii* and *S. solfataricus* UPRTases. Under the assumption of identical sites for binding of GTP in the two enzymes, the arginine residue (Arg34) providing specificity for the guanine nucleotide base is conserved. In other UPRTases, Arg34 is replaced with a glutamate residue. The superposition of the T.g.-UPRTase−GTP with the S.s.-UPRTase−UMP structure shows that the residues Lys95, Asp69, and Leu70 from the latter structure would make clashes with the guanine base and the ribosyl moiety of GTP. Assuming that the site for GTP binding is conserved among the UPRTases, binding of GTP to the *S. solfataricus* UPRTase must be associated with structural changes of the quaternary structure in line with the sigmoidal shape of the GTP binding and activation curves (*11*).

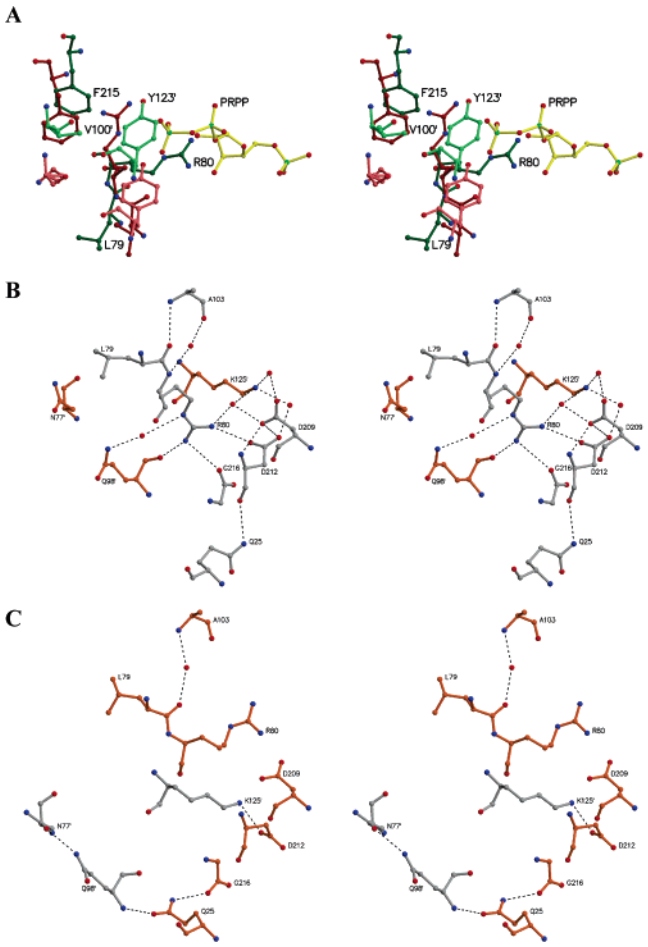

FIGURE 4: Illustrations of the environment of Arg80. (A) Superposition of T.g.-UPRTase−uracil−cPRPP (pink, red, and yellow) and S.s.-UPRTase−UMP−CTP (green). (B) Stereoview of Arg80 in the cis subunits of S.s.-UPRTase−UMP. (C) Stereoview of Arg80 in the trans subunits of S.s.-UPRTase−UMP.

Role of the C-Terminal Glycine. Cis−trans isomerization of the peptide bond between the first and second residues in the PP_i loop has been observed in other type-1 PRTases in response to binding of PRPP or PP_i (*32*, *38*), but the two different conformations have not previously been observed coexisting in the same enzyme. The conformation of the Arg80 side chain and therefore also its interactions depend on the conformation of the Leu79-Arg80 peptide bond. With the cis peptide bond present, a hydrogen bond is formed between Arg80 Nη and the C-terminal carboxylic acid group of Gly216 (Figure 4B). In the other UPRTases, this conserved glycine residue is followed by two or more residues (Figure 1). Corresponding hydrogen bonds are seen in *T. gondii* and *B. caldolyticus* UPRTase; however, in these

cases, Arg80 Nη interacts with the side-chain hydroxyl group from the subsequent threonine with the oxygen atom situated in almost the same position as the oxygen atoms from the C-terminal carboxyl group of Gly216. Gly216 adopts another conformation in the trans subunit, and one of the oxygen atoms of the terminal carboxyl group forms an indirect hydrogen bond with side chain of Gln98 in the cis subunit across the dimer−dimer interface (Figure 4C). In the subunits of S.s.-UPRTase−UMP−CTP, Gly216 is in the same conformation and makes the same interactions as Gly216 in the trans subunit. The interactions made by the C-terminal carboxyl group are clearly of importance for the control of enzyme activity. This was apparent from the kinetic studies of the *S. solfataricus* UPRTase with the C-terminal His tag. The attachment of six histidine residues to the C terminal of the protein results in enhancement of the k_{cat} of the unstimulated enzyme, while k_{cat} of the GTP-stimulated enzyme is unchanged and inhibition by CTP is retained (unpublished results). This indicates that the C-terminal His tag stabilizes the enzyme in a more active form, presumably by influencing the interactions made by the oxygen atoms of the carboxyl group of Gly216. The His tag probably also reduces the flexibility of the Gly216. In the trans subunit, one of oxygen atoms of the C-terminal carboxyl group makes indirect hydrogen bonds to N of Gln98 in the cis subunit across the dimer−dimer interface. Gln98 is situated in the beginning of the flexible loop, and therefore, it is likely that differences in the interactions made with Gln98 influence the stability of the flexible loop. The conformation of Gly216 in the trans subunit and the indirect hydrogen bond made to Gln98 may enhance the stability of a closed flexible loop in the adjacent subunit and thereby slow the access to the active site. If the intersubunit interactions between Gly216 and Gln98 result in impaired access to the active site, then this could explain the endogenous activation of the His-tagged enzyme, because these interactions may not be present in this enzyme.

CONCLUSION

The structural investigations show that Arg80 has a novel function in *S. solfataricus* UPRTase and plays a key role in the inhibition of the enzyme by the allosteric inhibitor CTP. Although this residue is conserved between different UPRTases, this important role in regulation is unique for *S. solfataricus* UPRTase. Also the C-terminal truncation of *S. solfataricus* UPRTase relative to other UPRTases seems to be essential for the development of the allosteric regulation, because the conformation and interactions of the C-terminal carboxyl group appear to influence the stability of the flexible loop in the adjacent subunit. Furthermore, both the kinetic characterization and the structural investigations indicate that a structural rearrangement of the enzyme is part of the catalytic mechanism. The structural studies further suggest that UPRTase utilizes a mechanism of ribosyl migration similar to other pyrimidine and purine PRTases.

ACKNOWLEDGMENT

We thank Lise Schack for the production and purification of the enzymes.

REFERENCES

1. Neuhard, J. (1983) Utilization of preformed pyrimidine bases and nucleosides, in *Metabolism of Nucleotides, Nucleosides, and Nucleobases in Microorganisms* (Munch-Petersen, A., Ed.) pp 95−148, Academic Press, London, U.K.
2. Schumacher, M. A., Carter, D., Scott, D. M., Roos, D. S., Ullman, B., and Brennan, R. G. (1998) Crystal structures of *Toxoplasma gondii* uracil phosphoribosyltransferase reveal the atomic basis of pyrimidine discrimination and prodrug binding, *EMBO J. 17*, 3219−3232.
3. Traut, T. W., and Jones, M. E. (1996) Uracil metabolism−UMP synthesis from orotic acid or uridine and conversion of uracil to β-alanine: Enzymes and cDNAs, *Prog. Nucleic Acid Res. Mol. Biol. 53*, 1−78.
4. Schumacher, M. A., Bashor, C. J., Song, M. H., Otsu, K., Zhu, S., Parry, R. J., Ullman, B., and Brennan, R. G. (2002) The structural mechanism of GTP stabilized oligomerization and catalytic activation of the *Toxoplasma gondii* uracil phosphoribosyltransferase, *Proc. Natl. Acad. Sci. U.S.A. 99*, 78−83.
5. Rasmussen, U. B., Mygind, B., and Nygaard, P. (1986) Purification and some properties of uracil phosphoribosyltransferase from *Escherichia coli* K12, *Biochim. Biophys. Acta 881*, 268−275.
6. Jensen, H. K., Mikkelsen, N., and Neuhard, J. (1997) Recombinant uracil phosphoribosyltransferase from the thermophile *Bacillus caldolyticus*: Expression, purification, and partial characterization, *Protein Expression Purif. 10*, 356−364.
7. Jensen, K. F., and Mygind, B. (1996) Different oligomeric states are involved in the allosteric behavior of uracil phosphoribosyltransferase from *Escherichia coli*, *Eur. J. Biochem. 240*, 637−645.
8. Kadziola, A., Neuhard, J., and Larsen, S. (2002) Structure of product-bound *Bacillus caldolyticus* uracil phosphoribosyltransferase confirms ordered sequential substrate binding, *Acta Crystallogr., Sect. D 58*, 936−945.
9. Joint Center for Structural Genomics, to be published, pdb code 1O5O.
10. Sinha, S. C., and Smith, J. L. (2001) The PRT protein family, *Curr. Opin. Struct. Biol. 11*, 733−739.
11. Jensen, K. F., Arent, S., Larsen, S., and Schack, L. Allosteric properties of the GTP activated and CTP inhibited uracil phosphoribosyltransferase from the thermo-acidophilic archaeon *Sulfolobus solfataricus*, *Eur. J. Biochem.* (in press).
12. Hendrickson, W. A., Horton, J. R., and LeMaster, D. M. (1990) Selenomethionyl proteins produced for analysis by multiwavelength anomalous diffraction (MAD): A vehicle for direct determination of three-dimensional structure, *EMBO J. 9*, 1665−1672.
13. Poulsen, J. C. N., Harris, P., Jensen, K. F., and Larsen, S. (2001) Selenomethionine substitution of orotidine-5′-monophosphate decarboxylase causes a change in crystal contacts and space group, *Acta Crystallogr., Sect. D 57*, 1251−1259.
14. Clark, D. J., and Maaloe, O. (1967) DNA replication and the division cycle in *Escherichia coli*, *J. Mol. Biol. 23*, 99−112.
15. Jancarik, J., and Kim, S. H. (1991) Sparse matrix sampling: A screening method for crystallization of proteins, *J. Appl. Crystallogr. 24*, 409−411.
16. Cerenius, Y., Ståhl, K., Svensson, L. A., Ursby, T., Oskarsson, Å., Albertsson, J., and Liljas, A. (2000) The crystallography beamline I711 at MAX II, *J. Synchotron Radiat. 7*, 203−208.
17. Otwinowski, Z., and Minor, W. (1997) Processing of X-ray diffraction data collected in oscillation mode, *Methods Enzymol. 276*, 307−326.
18. French, S., and Wilson, K. (1978) Treatment of negative intensity observations, *Acta Crystallogr., Sect. A 34*, 517−525.
19. Terwilliger, T. C., and Berendzen, J. (1999) Automated MAD and MIR structure solution, *Acta Crystallogr., Sect. D 55*, 849−861.
20. Bricogne, G., Vonrhein, C., Flensburg, C., Schiltz, M., and Paciorek, W. (2003) Generation, representation, and flow of phase information in structure determination: Recent developments in and around SHARP 2.0, *Acta Crystallogr., Sect. D 59*, 2023−2030.
21. Terwilliger, T. C. (1999) Reciprocal-space solvent flattening, *Acta Crystallogr., Sect. D 55*, 1863−1871.
22. Jones, T. A., Zou, J. Y., Cowan, S. W., and Kjeldgaard, M. (1991) Improved methods for building protein models in electron density maps and the location of errors in these models, *Acta Crystallogr., Sect. A 47*, 110−119.
23. Brünger, A. T., Adams, P. D., Clore, G. M., DeLano, W. L., Gros, P., GrosseKunstleve, R. W., Jiang, J. S., Kuszewski, J., Nilges, M., Pannu, N. S., Read, R. J., Rice, L. M., Simonson, T., and Warren, G. L. (1998) Crystallography and NMR system: A new

software suite for macromolecular structure determination, *Acta Crystallogr., Sect. D 54*, 905−921.
24. Navaza, J. (1994) AMoRe: An automated package for molecular replacement, *Acta Crystallogr., Sect. A 50*, 157−163.
25. Laskowski, R. A., MacArthur, M. W., Moss, D. S., and Thornton, J. M. (1993) PROCHECK: A program to check the stereochemical quality of protein structures, *J. Appl. Crystallogr. 26*, 283−291.
26. Kraulis, P. J. (1991) MOLSCRIPT: A program to produce both detailed and schematic plots of protein structures, *J. Appl. Crystallogr. 24*, 946−950.
27. Merritt, E. A., and Bacon, D. J. (1997) Raster3D: Photorealistic molecular graphics, *Methods Enzymol. 277*, 505−524.
28. Madsen, D., Johansson, P., Johansson, N., Arent, S., Harris, M. R., and Kleywegt, G. J. INDONESIA: An integrated workbench for sequence and structure alignment and analysis, manuscript submitted.
29. Lundegaard, C., and Jensen, K. F. (1999) Kinetic mechanism of uracil phosphoribosyltransferase from *Escherichia coli* and catalytic importance of the conserved proline in the PRPP binding site, *Biochemistry 38*, 3327−3334.
30. Wriggers, W., and Schulten, K. (1997) Protein domain movements: Detection of rigid domains and visualization of hinges in comparisons of atomic coordinates, *Proteins: Struct., Funct., Genet. 29*, 1−14.
31. Seshadri, T. P., Viswamitra, M. A., and Kartha, G. (1980) Structure of disodium uridine 5′-phosphate heptahydrate, *Acta Crysallogr., Sect. B 36*, 925−927.
32. Shi, W., Sarver, A. E., Wang, C. C., Tanaka, K. S. E., Almo, S. C., and Schramm, V. L. (2002) Closed site complexes of adenine phosphoribosyltransferase from *Giardia lamblia* reveal a mechanism of ribosyl migration, *J. Biol. Chem. 277*, 39981−39988.
33. Héroux, A., White, E. L., Ross, L. J., Kuzin, A. P., and Borhani, D. W. (2000) Substrate deformation in a hypoxanthine-guanine phosphoribosyltransferase ternary complex: The structural basis for catalysis, *Structure 8*, 1309−1318.
34. Tao, W., Grubmeyer, C., and Blanchard, J. S. (1996) Transition state structure of *Salmonella typhimurium* orotate phosphoribosyltransferase, *Biochemistry 35*, 14−21.
35. Xu, Y., Eads, J., Sacchettini, J. C., and Grubmeyer, C. (1997) Kinetic mechanism of human hypoxanthine-guanine phosphoribosyltransferase: Rapid phosphoribosyl transfer chemistry, *Biochemistry 36*, 3700−3712.
36. Wang, G. P., Cahill, S. M., Liu, X., Girvin, M. E., and Grubmeyer, C. (1999) Motional dynamics of the catalytic loop in OMP synthase, *Biochemistry 38*, 284−295.
37. Wang, G. P., Lundegaard, C., Jensen, K. F., and Grubmeyer, C. (1999) Kinetic mechanism of OMP synthase: A slow physical step following group transfer limits catalytic rate, *Biochemistry 38*, 275−283.
38. Héroux, A., White, E. L., Ross, L. J., Davis, R. L., and Borhani, D. W. (1999) Crystal structure of *Toxoplasma gondii* hypoxanthine-guanine phosphoribosyltransferase with XMP, pyrophosphate, and two Mg^{2+} ions bound: Insights into the catalytic mechanism, *Biochemistry 38*, 14495−14506.

BI048041L